

Numerical Analysis on Stagnation Point Flow of Micropolar Nanofluid with Thermal Radiations over an Exponentially Stretching Surface

FERAS M. AL FAQIH¹, KHURAM RAFIQUE², SEHAR ASLAM², MOHAMMED Z. SWALMEH³

¹Department of Mathematics,
Al-Hussein Bin Talal University,
Ma'an 71111,
JORDAN

²Department of Mathematics,
University of Sialkot,
Sialkot 51310,
PAKISTAN

³Faculty of Arts and Sciences,
Aqaba University of Technology,
Aqaba 77110,
JORDAN

Abstract: - Several industrial developments such as polymer extrusion in metal spinning and continuous metal casting include energy transmission and flow over a stretchy surface. In this paper, the stagnation point flow of micropolar nanofluid over a slanted surface is presenting also considering the influence of thermal radiations. Buongiorno's nanofluid model is deployed to recover the thermophoretic effects. By using similarity transformations, the governing boundary layer equations are transformed into ordinary differential equations. The Keller-box approach is used to solve transformed equations numerically. The numerical outcomes are presented in tabular and graphical form. A comparison of the outcomes attained with previously published results is done after providing the entire formulation of the Keller-Box approach for the flow problem under consideration. It has been found that the reduced Sherwood number grows for increasing values of radiation parameter while, reduced Nusselt number and skin friction coefficient decreases. Furthermore, the skin-friction coefficient increases as the inclination factor increases, but Nusselt and Sherwood's numbers decline.

Keywords: - Micropolar nanofluid, Stretching sheet, Stagnation point flow, Thermal Radiations, Keller-Box Technique.

Received: January 26, 2023. Revised: November 15, 2023. Accepted: December 14, 2023. Published: February 1, 2024.

1 Introduction

The concept of nanofluids is not new, [1], initially proposed it when they were looking for new coolants and cooling technologies. It quickly gained popularity due to its many uses in nuclear reactor systems, heat exchangers, electronic cooling, boilers, and energy storage devices. A fluid called a nanofluid contains microscopic quantities of nanoparticles or nanofibers, which are particles with a diameter of less than 100 nm. Emerging heat transfer base fluids including water, ethylene glycol, toluene, and motor oil are mixed with nanoparticles or nanofibers to create nanofluids. [2], investigated the base fluid's thermal conductivity may be increased by the inclusion of nanoparticles, which is expected to increase the free

convection heat transfer of the nanofluid relative to the base fluid. The capability to conduct heat is increased by up to 60% when added CuO nanoparticles to a base liquid, with a volume proportion of 5%, according to a study by [3]. Additionally, they claimed that adding a 1% volume fraction of copper nanoparticles to the regular fluid boosted heat conductivity by up to 40%. In his research, [4], identified seven pathways that are crucial for improving the base fluid's thermal conductivity. The two most important of these processes are thermophoresis and Brownian motion. He concluded that due to the impact of the temperature differential and thermophoresis, the boundary layer's nanofluid characteristics may differ dramatically. These effects can significantly reduce the viscosity inside the boundary layer for a heated fluid, improving

heat transmission. [5], examined the key elements that might improve thermal conductivity. It has been shown that several variables, including particle size and shape, base fluids, fluid PH, temperature, surfactant type, hydrogen bonding, solvent type, and others, directly affect how well nanofluids transmit heat. On the other hand, viscosity is one of the other elements that affects heat conductivity in an "indirect" manner.

A stretched sheet's boundary layer flow has various technical applications, including skin friction, grain storage, paper manufacturing, and drag reduction. The initial study was done by [6], on the boundary layer flow with unchanged velocity over a continuous solid surface. Further, [7], studied and published closed-form solutions for the boundary layer flow of a viscous fluid through a stretched surface. [8], investigated the impact of nonlinear radiation and heat generation or absorption on the flow of nanofluid at its stagnation point along a moving surface. Coupled nonlinear PDEs were converted into nonlinear coupled ODEs using similarity transformations, and a finite difference method was then used to derive the unknown functions for velocity, temperature, and nanoparticle concentration. [9], talks about the microorganism-containing nanofluid's stagnation point flow. By using suitable transformation, the system of pde's was transformed into a system of ode's, and the resulting equations were then solved numerically using the bvp4c MATLAB tool. [10], researched micropolar nanofluid stagnation point flow for slanted surfaces.

Micropolar fluids are fluids made up of randomly oriented and rigid particles suspended in a viscous medium with micro-structure components. To investigate the impact of micro rotations on fluid motion, [11], [12], established the theory of micropolar fluids. [13], used a fluid model to undertake numerical analysis on incompressible, time-dependent electrically-conducting squeezing flow/micropolar fluid. Slip parameters were found to down the value of the Nusselt and Sherwood numbers on both discs. [14], used a computational model to investigate the mass and energy transport behavior of micro-rotational flow through a Riga-plate, taking into account suction or injection as well as mixed convection. [15], investigated hydromagnetic micropolar nanofluid flow via a nonlinear stretchy sheet and generated entropy using Navier slips. The results demonstrated that when the Brownian motion was increased, the momentum boundary layer improved while, the concentration distribution decreased. Results of several recent researches on micropolar nanofluid flow are presented in the studies, [16], [17], [18], [19], [20], [21], [22], [23], [24], [25].

Nanotechnology has gained a prominent place in the current era research area due to which nanoliquid becomes a very important liquid that trigger the thermal efficiency of base liquids. The higher thermal efficiency ability is very helpful in energy transportation. The literature previously mentioned inspired us to explore the stagnation point flow of the micro-polar nanofluid towards a sloping surface with Brownian motion and the Thermophoretic impacts. However, no researcher has to date taken into account the slanted surface for the stagnation point flow of micro-rotational nanofluid by incorporating the considered effects, using the Keller box method. We subsequently carried out this analysis to fill this gap in the literature. There are different methods that can utilize to find the numerical and graphical results of the current research but the Keller box technique is easier for simulation and to prepare the Matlab program. Further this method is very friendly to use and gives more accurate results. Moreover, Figure 1 presents the physical Model and Coordinate System of the utilized study.

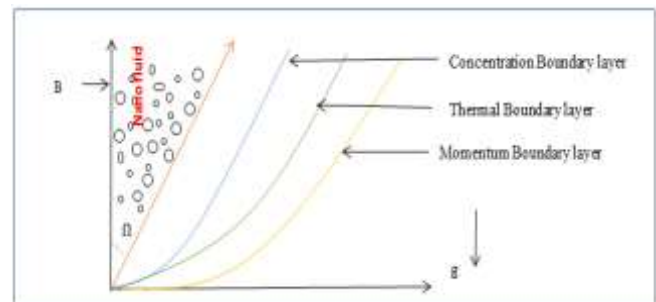


Fig. 1: Physical Model and Coordinate System

2 Problem Formulation

In this study micro-rotation of the incompressible nanoliquid flow is considered. The rotational effects of micropolar liquid along with nanoparticles are investigated. We examine a micropolar nanofluid's two-dimensional stagnation-point flow towards a slanted exponentially stretchable sheet. Additionally, $B(x) = B_0 e^{\frac{x}{l}}$ (magnetic field) along with inclination effects are under examination. In this problem, the stretching and free stream velocity's are taken as $u_w(x) = a e^{x/l}$ and $u \rightarrow u_\infty(x) = b e^{x/l}$ where, a and b both are constants and x is the axis measured along the stretching surface. Along with nanoparticles, the base fluid also contains rotating micropolar finite-sized particles. At the wall, T and C remain constant and are denoted by the letters T_w and C_w , where T stands for temperature and C for the nanoparticle fraction.

The equations that govern boundary layers given the reference, [26], [27], [28], are,

$$\frac{\partial u}{\partial x} + \frac{\partial v}{\partial y} = 0, \quad (1)$$

$$u \frac{\partial u}{\partial x} + v \frac{\partial u}{\partial y} = u_\infty \frac{du_\infty}{dx} + \left(\frac{\mu+k_1^*}{\rho}\right) \frac{\partial^2 u}{\partial y^2} + \left(\frac{k_1^*}{\rho}\right) \frac{\partial N^*}{\partial x} + \frac{\sigma B^2}{\rho} (u_\infty - u) + g[\beta_t(T - T_\infty) + \beta_c(C - C_\infty)] \cos \Omega, \quad (2)$$

$$\frac{\partial N^*}{\partial x} + v \frac{\partial N^*}{\partial y} = \left(\frac{\gamma^*}{j^* \rho}\right) \frac{\partial^2 N^*}{\partial y^2} - \left(\frac{k_1^*}{j^* \rho}\right) \left(2N^* + \frac{\partial u}{\partial y}\right), \quad (3)$$

$$u \frac{\partial T}{\partial x} + v \frac{\partial T}{\partial y} = \alpha \frac{\partial^2 T}{\partial y^2} - \frac{1}{(\rho c)_f} \frac{\partial q_r}{\partial y} + \tau \left[D_B \frac{\partial C}{\partial y} \frac{\partial T}{\partial y} + \frac{D_T}{T_\infty} \left(\frac{\partial T}{\partial y}\right)^2 \right], \quad (4)$$

$$u \frac{\partial C}{\partial x} + v \frac{\partial C}{\partial y} = D_B \frac{\partial^2 C}{\partial y^2} + \frac{D_T}{T_\infty} \frac{\partial^2 T}{\partial y^2}. \quad (5)$$

The Rosseland approximation is used to simplify the equation (4), which reduces the radiative heat flux to:

$$q_r = \frac{-4\sigma^* \partial T^4}{3k^* \partial y}, \quad (6)$$

Where, respectively, σ^* and k^* represents the Stefan-Boltzmann constant and the mean absorption coefficient. Ignoring higher-order terms, extending about T_∞ , T^4 in a Taylor series results in:

$$T^4 = 4T_\infty^3 T - 3T_\infty^4,$$

Thus, simplified form of equation (4) is:

$$u \frac{\partial T}{\partial x} + v \frac{\partial T}{\partial y} = \alpha \left(1 + \frac{4N}{3}\right) \frac{\partial^2 T}{\partial y^2} + \tau \left[D_B \frac{\partial C}{\partial y} \frac{\partial T}{\partial y} + \frac{D_T}{T_\infty} \left(\frac{\partial T}{\partial y}\right)^2 \right], \quad (7)$$

Where u and v both are velocity components in x and y directions resp., σ depicts the electrical conductivity, ρ represents base fluid's density, μ denotes viscosity, γ^* shows spin gradient viscosity, k_1^* depicts vertex viscosity, j^* denotes micro-inertia per unit mass, the thermal diffusivity parameter is $\alpha = \frac{k}{(\rho c)_f}$ where, $(\rho c)_f$ is the heat capacity of base fluid and k is known as thermal conductivity, N represents radiation parameter, $\tau = \frac{(\rho c)_p}{(\rho c)_f}$ is the relation between heat capacity of nanoparticles and of liquids, furthermore, D_T stands for thermophoresis diffusion coefficient and D_B stands for Brownian motion.

Boundary conditions that are imposed in view of [27], [28], are listed below.

$$u = u_w(x) = ae^{x/l}, v = 0, N^* = -n_0 \frac{\partial u}{\partial y}, T = T_w(x), C = C_w(x) \text{ at } (y = 0),$$

$$u \rightarrow u_\infty = be^{x/l}, v \rightarrow 0, N^* \rightarrow 0, T \rightarrow T_w, C \rightarrow C_w \text{ as } y \rightarrow \infty. \quad (8)$$

When, $n_0 = 0$, it is implied that $N^* = 0$ at the wall, which stands for concentrated outline flow and deny the rotation of micro-elements along the surface of wall. In order to convert the nonlinear PDE's into nonlinear ODE's, similarity transformations are defined. The stream function $\sigma\psi = \psi(x, y)$ is defined as follows for this use:

$$u = \frac{\partial \psi}{\partial y}, v = -\frac{\partial \psi}{\partial x}. \quad (9)$$

The exponentially stretching sheet velocity is used to define the similarity transformations given, [27], [28], as follows:

$$\psi = \sqrt{2lva} e^{\frac{x}{2l}} f(\eta), N^* = \left(\frac{a}{2\gamma l}\right) e^{\frac{3x}{2l}} \sqrt{2lva} h(\eta), \\ \theta(\eta) = \frac{T - T_\infty}{T_w - T_\infty}, \phi(\eta) = \frac{C - C_\infty}{C_w - C_\infty}. \quad (10)$$

Where,

$$T_w = T_\infty + T_0 e^{\frac{x}{2l}}, C_w = C_\infty + C_0 e^{\frac{x}{2l}}.$$

Equations (2, 3, 5 and 7) are converted to the following nonlinear ODE's when Eq. (10) is substituted:

$$(1 + K)f'''' + ff'' - 2f'^2 + 2\gamma^2 + Kh' + M(\gamma - f') + (\lambda\theta + \delta\phi)\cos\Omega = 0, \quad (11)$$

$$\left(1 + \frac{K}{2}\right)h'' + h'f - 3f'h - K(2h + f'') = 0, \quad (12)$$

$$\left(1 + \frac{4}{3}N\right)\theta'' + (\theta'f - \theta f' + Nb\theta'\phi' + Nt\theta'^2)Pr = 0, \quad (13)$$

$$\phi'' + Le(\phi'f - \phi f') + \frac{Nt}{Nb}\theta'' = 0, \quad (14)$$

Where,

$$\gamma = \frac{b}{a}, Pr = \frac{\nu}{\alpha}, Le = \frac{\nu}{D_B}, M = \frac{2\sigma B_0^2}{a\rho}, K = \frac{k_1^*}{\mu}, Nb = \frac{D_B \tau (C_w - C_\infty)}{\nu}, Nt = \frac{\tau D_T (T_w - T_\infty)}{\nu T_\infty}, Nt_b = \frac{Nt}{Nb}, \lambda = \frac{G_r}{Re_x^2}, G_r = \frac{2gB_t(T_w - T_\infty)l^3}{\nu^2}, \delta = \frac{G_c}{Re_x^2}, G_c = \frac{2gB_c(C_w - C_\infty)l^3}{\nu^2}, Le = \frac{\nu}{D_B}, N = \frac{4\sigma T_\infty^3}{kk^*}. \quad (15)$$

Here, prime denotes derivatives w.r.t η , M represents magnetic parameter, the Prandtl number is depicted by Pr , K depicts dimensionless vortex viscosity, γ velocity ratio parameter, N is radiation parameter, ν is kinematic viscosity of the fluid, the Lewis number is Le , $Nt_b = \frac{Nt}{Nb}$ where, Nt is thermophoresis parameter and Nb is Brownian motion parameter, λ is buoyancy parameter and G_r is local Grashof number, δ is solutal buoyancy parameter and G_c is local Grashof number. The imposed boundary conditions (8) are transformed to

$$f'(\eta) = 1, f(\eta) = 0, h(\eta) = -n_0 f''(\eta), \theta(\eta) = 1, \phi(\eta) = 1, \text{ at } \eta = 0, \\ f'(\eta) \rightarrow \gamma, \theta(\eta) \rightarrow 0, h(\eta) \rightarrow 0, \phi(\eta) \rightarrow 0 \text{ as } \eta \rightarrow \infty. \quad (16)$$

The Sherwood number (Sh), the coefficient of skin friction (C_{fx}) and the Nusselt number (Nu) are defined as:

$$Sh = \frac{xq_m}{D_B(C_w - C_\infty)}, Nu = \frac{xq_w}{k(T_w - T_\infty)}, C_{fx} = \frac{\tau_w}{\rho u_w^2} \quad (17)$$

Where, $\tau_w = (\mu + k_1^*) \frac{\partial u}{\partial y} + k_1^* N^*$, $q_w = -k \frac{\partial T}{\partial y}$ and $q_m = -D_B \frac{\partial c}{\partial y}$ at $y = 0$

The relations of the coefficient of skin friction $C_{fx}(0) = (1 + K)f''(0)$, the reduced Sherwood number $-\phi'(0)$ and the reduced Nusselt number $-\theta'(0)$ are defined as:

$$C_{fx}(0) = C_f \sqrt{Re_x}, -\phi'(0) = \frac{Sh}{\sqrt{Re_x}}, -\theta'(0) = \frac{Nu}{(1 + \frac{4}{3}N)\sqrt{Re_x}} \quad (18)$$

Here, the local Reynolds number is $Re_x = \frac{ax e^{x/t}}{\nu}$.

3 Results and Discussion

The Keller-box approach is used to solve the transformed nonlinear ODE's (11–14) that are subjected to BC's (16). The results for the relevant physical parameters, such as $Nb, Pr, M, N, \delta, \Omega, Nt, Le, K, \lambda$, and γ are presented in tabular form by using tables 1 and 2. When $\delta, Nt, K, \gamma, Nb, \lambda$, and Le are equal to zero and $\Omega = 90^0$. Table 1 compares the current findings for the reduced Nusselt number $-\theta'(0)$ to the findings from, [26] and [27]. Here, a good consensus can be seen. In this work Keller box technique utilized. Since last few years, this numerical technique is very effective and accomplished of making correct numerical results of the flow problems by being categorically stable up to second-order convergence. This technique is very friendly in use and coding, easy to program, and give unconditional convergence in reasonable time at second order.

Table 1. Comparison of $-\theta'(0)$ when $\delta, Nb, Nt, \lambda, K, Le, \gamma = 0$ and $\Omega = 90^0$.

<i>Pr</i>	<i>M</i>	<i>N</i>	Bidin and Nazar [26]	Ishak [27]	Present results
			$-\theta'(0)$	$-\theta'(0)$	$-\theta'(0)$
1.0	0	0	0.9548	0.9548	0.9548
2.0	0	0	1.4714	1.4714	1.4714
3.0	0	0	1.8691	1.8691	1.8691
1.0	0	1.0	0.5312	0.5312	0.5312
1.0	1.0	0	--	0.8611	0.8611
1.0	1.0	1.0	--	0.4505	0.4505

Table 2. Values of $-\theta'(0), -\phi'(0)$ and $C_{fx}(0)$.

<i>Nb</i>	<i>Nt</i>	<i>Pr</i>	<i>Le</i>	<i>M</i>	<i>K</i>	<i>N</i>	λ	δ	γ	Ω	$-\theta'(0)$	$-\phi'(0)$	$C_{fx}(0)$
0.1	0.1	6.5	5.0	0.1	1.0	1.0	0.1	0.1	0.5	45 ⁰	0.8984	2.5492	1.1925
0.3	0.1	6.5	5.0	0.1	1.0	1.0	0.1	0.1	0.5	45 ⁰	0.6010	2.6985	1.1930
0.1	0.3	6.5	5.0	0.1	1.0	1.0	0.1	0.1	0.5	45 ⁰	0.7167	2.6100	1.1859
0.1	0.1	9.0	5.0	0.1	1.0	1.0	0.1	0.1	0.5	45 ⁰	0.9902	2.5505	1.1949
0.1	0.1	6.5	9.0	0.1	1.0	1.0	0.1	0.1	0.5	45 ⁰	0.8701	3.8017	1.1979
0.1	0.1	6.5	5.0	0.5	1.0	1.0	0.1	0.1	0.5	45 ⁰	0.8943	2.5407	1.2716
0.1	0.1	6.5	5.0	0.1	3.0	1.0	0.1	0.1	0.5	45 ⁰	0.9188	2.5914	1.6193
0.1	0.1	6.5	5.0	0.1	1.0	3.0	0.1	0.1	0.5	45 ⁰	0.6908	2.5851	1.1879
0.1	0.1	6.5	5.0	0.1	1.0	1.0	0.5	0.1	0.5	45 ⁰	0.9030	2.5591	1.0894
0.1	0.1	6.5	5.0	0.1	1.0	1.0	0.1	1.0	0.5	45 ⁰	0.9051	2.5638	1.0230
0.1	0.1	6.5	5.0	0.1	1.0	1.0	0.1	0.1	1.5	45 ⁰	1.0615	2.8750	-1.7549
0.1	0.1	6.5	5.0	0.1	1.0	1.0	0.1	0.1	0.5	60⁰	0.8978	2.5480	1.2057

To illustrate how $\theta'(0)$, $\phi'(0)$, and $C_{fx}(0)$ vary for different values of Le , Pr , M , N , δ , Ω , Nt , Nb , K , λ and γ , Table 2 is constructed. It has been found that when, Nb , N , Nt , M and Ω are increased, $\theta'(0)$ lowers, whereas Pr , λ , γ , K and δ are increased, $\theta'(0)$ grows. The table, however, clearly demonstrates that $\phi'(0)$ is decreasing while rising Ω , and M . While, rising with higher values of K , Pr , Nt , γ , Nb , N , λ , δ and Le . Additionally, it has been discovered that $C_{fx}(0)$ decreases as Nt , λ , N and δ increases when Nb , Le , K , M , Ω , and Pr increases values rise. The negative values of $C_{fx}(0)$ signify a drag force being applied to the motions of the micropolar nanofluid by the stretching sheets. This is not unexpected considering that stretching is the only factor responsible for the boundary layer's development. It can be seen from this table that the increasing value of γ gives higher values of $C_{fx}(0)$. Logically the inclination factor improves the skin friction. Further it is seen clearly from Table 2 the increment in the magnetif effect the energy and mass transmission rates diminishes. Physically the magnetic causes reduction in the speed of the liquid. Moreover, the effect of the magnetic field (M) on the velocity outline for $\gamma < 1$ and $\gamma > 1$ is depicted in Figure 2. It demonstrates that as the strength of the magnetic field is increased, $f'(\eta)$ decreases for $\gamma < 1$ and increases for $\gamma > 1$. This figure matched with already published research work of Alkansasbeh [29] which validatesur current utilized numerical method. Additionally, as seen in Figure 3, $f'(\eta)$ gets better with the growth of γ for both $\gamma < 1$ and $\gamma > 1$. This occurs because a boundary layer forms in the flow when $\gamma > 1$, or the free stream velocity, exceeds the stretchable velocity. Physically, the fluid motion increases as it approaches the point of stagnation, which increases the external stream's acceleration. In turn, as rises, the boundary layer thickness decreases. On the other hand, a reversed boundary layer develops when the velocity of the stream is lower than that of the stretching, or $\gamma < 1$.

However, both velocities are identical and there is no boundary layer when $\gamma = 1$. Figure 4 depicts the behaviour of the temperature profile in relation to the radiation parameter (N). As the radiation parameter increases, the temperature profile rises, which causes the flow field to produce heat and raise the temperature of the thermal boundary layer. Figure 5 represents the effects of Brownian motion parameter on term. Profile for $\gamma < 1$ and $\gamma > 1$. The temperature profile rises in response to rising values of Nb . Figure 6 compares and shows the effects of thermophoresis on the temperature profile against $\gamma < 1$ and $\gamma > 1$. The thermophoresis effect demonstrates a direct interaction with the temperature field. Logically the increase in

Brownian motion factor enhances the movement of particles which cacauseshe growth of temperature. Figure 7 shows how a change in prandtl number results in a drop in temperature and a corresponding reduction in boundary layer thickness. Figure 8 describes the thermophoretic effect on $\phi(\eta)$ for $\gamma < 1$ and $\gamma > 1$. From the sketch, it is clear that the concentration is reduced for changed values of Nt . A decrease.in boundary layer thickness caused by an increase.in Nb . against $\gamma < 1$ and $\gamma > 1$ results in a decrease.in the concentration profile (Figure 9). Figure 10 demonstrates how the concentration.outline drops off as Le increases. It is due to the decrease in boundary stream viscosity against increment in Le .

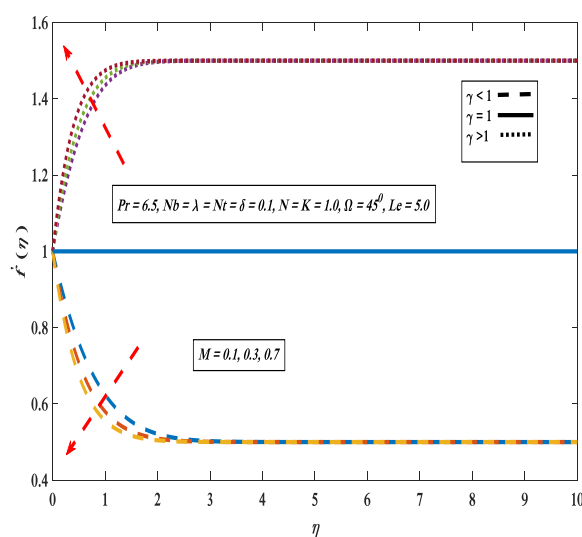


Fig. 2: Variation of $f'(\eta)$ via Magnetic parameter

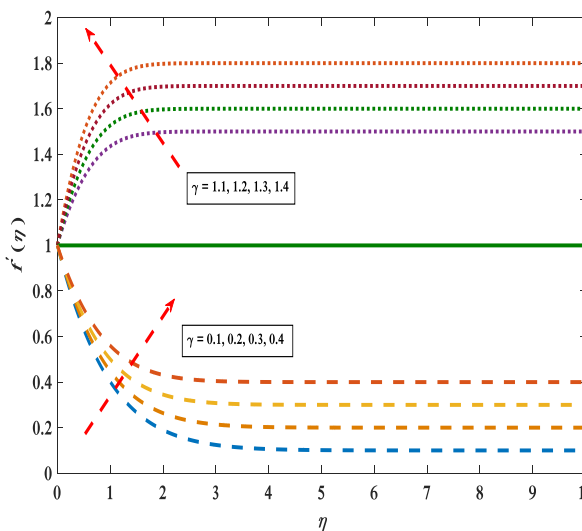


Fig. 3: Variation of $f'(\eta)$ via Velocity ratio parameter

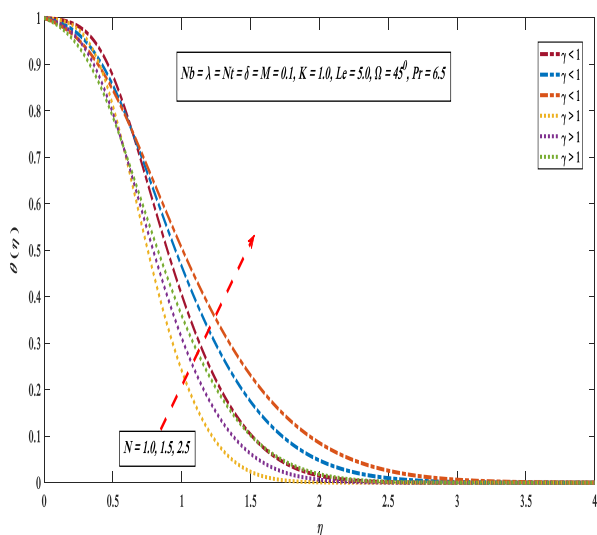


Fig. 4: Variation of $\theta'(\eta)$ via Radiation parameter

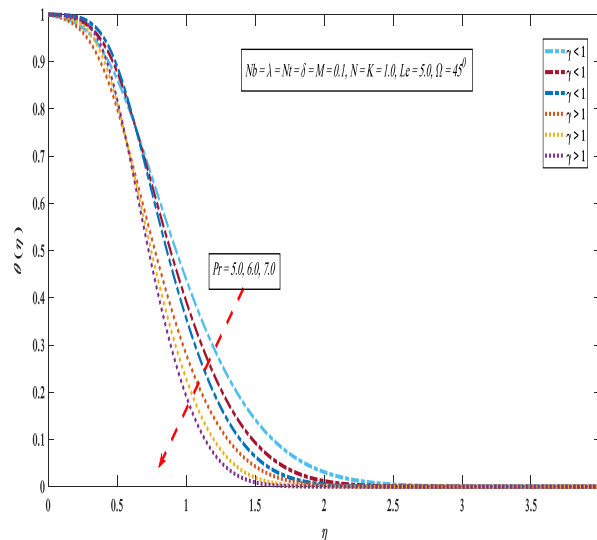


Fig. 7: Variation of $\theta'(\eta)$ via Prandtl number

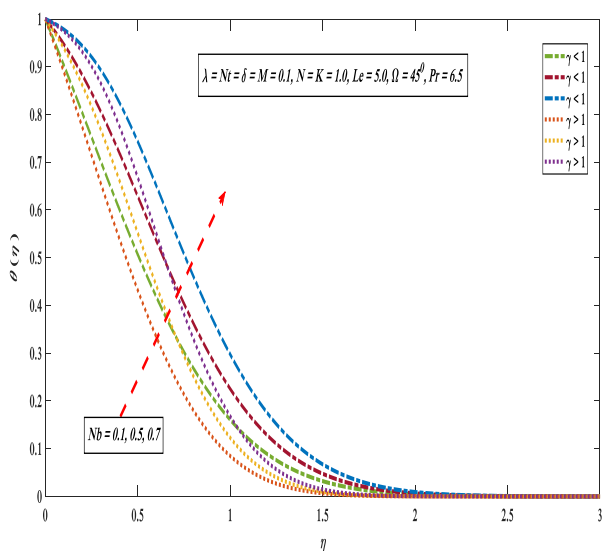


Fig. 5: Variation of $\theta'(\eta)$ via Brownian motion parameter

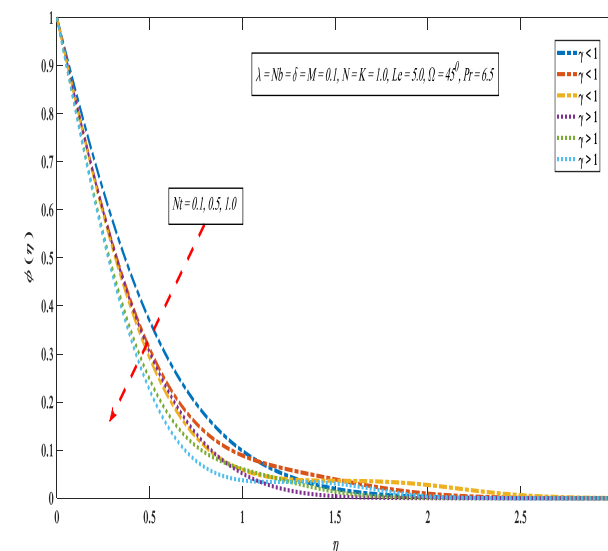


Fig. 8: Variation of $\phi'(\eta)$ via Thermophoresis parameter

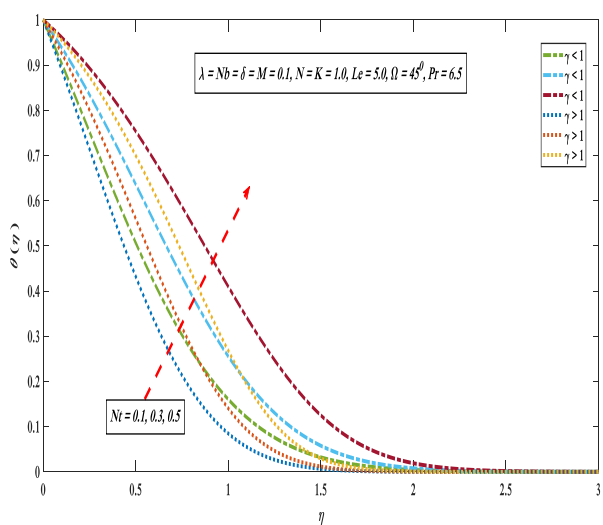


Fig. 6: Variation of $\theta'(\eta)$ via Thermophoresis parameter

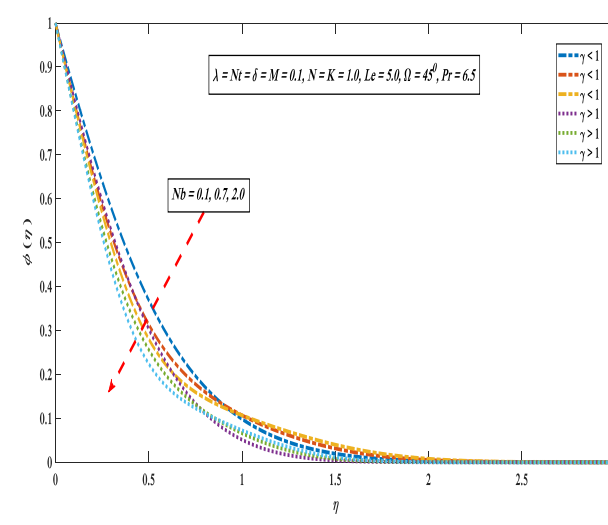


Fig. 9: Variation of $\phi'(\eta)$ via Brownian motion parameter

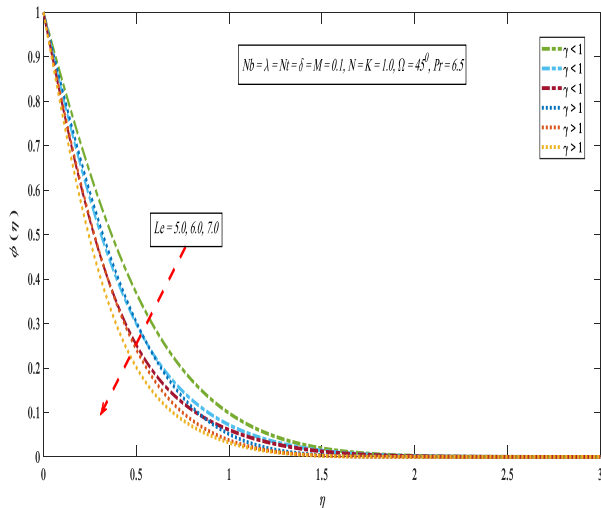


Fig. 10: Variation of $\phi'(\eta)$ via Lewis number

4 Conclusions

The investigation of the stagnation point flow of a micropolar nanofluid toward an inclined exponential stretching surface has been examined in this article. The impacts of Brownian motion and thermophoresis are incorporated in the flow field. Moreover, the radiation impact has been considered in this investigation. The micro-rotational effects on the nanoliquid discussed. Additionally, the stagnation flow by incorporating magnetic factor has been discussed numerically with Keller box scheme. The following are the key findings of this study.

when Nb , Nt , M and Ω are increased, $-\theta'(0)$ lowers, whereas Pr , λ , γ , K and δ are increased, $-\theta'(0)$ grows.

Radiation parameter diminishes the energy transportation with growing values.

$-\phi'(0)$ is decreasing while rising Ω and M .

$C_{fx}(0)$ decreases as, N and δ increases,

$-\phi'(0)$ increases for increasing values of (N) while $-\theta'(0)$ and $C_{fx}(0)$ decreases.

$C_{fx}(0)$ increases as the inclination factor (Ω) increases.

$-\phi'(0)$ and $-\theta'(0)$ enhances by the growth in inclination. In the future, this work can be extended for different geometries, for instance, disk, cylinder, sphere, etc.

References:

[1] Choi, S. U., & Eastman, J. A. (1995). Enhancing thermal conductivity of fluids with nanoparticles (No. ANL/MSD/CP-84938; CONF-951135-29). Argonne National Lab.(ANL), Argonne, IL (United States).

[2] Alshomrani, A. S., Sivasankaran, S., & Ahmed, A. A. (2020). Numerical study on convective flow and heat transfer in a 3D inclined enclosure with hot solid body and discrete cooling. *International Journal of Numerical Methods for Heat & Fluid Flow*, Vol. 30 No. 10, pp. 4649-4659. <https://doi.org/10.1108/HFF-09-2019-0692>.

[3] Eastman, J. A., Choi, U. S., Li, S., Thompson, L. J., & Lee, S. (1996). Enhanced thermal conductivity through the development of nanofluids. *MRS Online Proceedings Library (OPL)*, 457.

[4] Buongiorno, J. (2006). Convective transport in nanofluids, *J. Heat Transfer*. Mar. 2006, 128(3): 240-250, <https://doi.org/10.1115/1.2150834>.

[5] Younes, H., Mao, M., Murshed, S. S., Lou, D., Hong, H., & Peterson, G. P. (2022). Nanofluids: Key parameters to enhance thermal conductivity and its applications. *Applied Thermal Engineering*, 118202.

[6] Sakiadis BC (1966) Boundary layer behavior on continuous solid surfaces: I. Boundary layer equations for two-dimensional and axisymmetric flow. *AIChE J* 7:26–28.

[7] Crane LJ (1970) *Flow past a stretching plate*. *Z Angew Math Physk*. 21:645–647.

[8] Soomro, F. A., Haq, R. U., Al-Mdallal, Q. M., & Zhang, Q. (2018). Heat generation/absorption and nonlinear radiation effects on stagnation point flow of nanofluid along a moving surface. *Results in Physics*, 8, 404-414.

[9] Al-Amri, F., & Muthamilselvan, M. (2020). Stagnation point flow of nanofluid containing micro-organisms. *Case Studies in Thermal Engineering*, 21, 100656.

[10] Rafique, K., Anwar, M. I., Misiran, M., Khan, I., Seikh, A. H., Sherif, E. S. M., & Nisar, K. S. (2019). Numerical analysis with Keller-box scheme for stagnation point effect on the flow of micropolar nanofluid over an inclined surface. *Symmetry*, 11(11), 1379.

[11] Eringen AC (1964) Simple micro fluids. *Int J Eng Sci.*, 2:205–217

[12] Eringen AC (1966) Theory of micropolar fluids. *J. Math Mech.*, 16:1–18

[13] Hussain, T., & Xu, H. (2022). Time-dependent squeezing bio-thermal MHD convection flow of a micropolar nanofluid between two parallel disks with multiple slip effects. *Case Studies in Thermal Engineering*, 31, 101850.

[14] Rafique, K., Alotaibi, H., Ibrar, N., & Khan, I. (2022). Stratified Flow of Micropolar Nanofluid over Riga Plate: Numerical Analysis. *Energies*, 15(1), 316.

- [15] Fatunmbi, E. O., & Salawu, S. O. (2022). Analysis of hydromagnetic micropolar nanofluid flow past a nonlinear stretchable sheet and entropy generation with Navier slips. *International Journal of Modelling and Simulation*, 42(3), 359-369.
- [16] Bafakeeh, O. T., Raghunath, K., Ali, F., Khalid, M., Tag-ElDin, E. S. M., Oreijah, M., & Khan, M. I. (2022). Hall current and Soret effects on unsteady MHD rotating flow of second-grade fluid through porous media under the influences of thermal radiation and chemical reactions. *Catalysts*, 12(10), 1233.
- [17] Ahmed, M. F., Zaib, A., Ali, F., Bafakeeh, O. T., Tag-ElDin, E. S. M., Guedri, K., ... & Khan, M. I. (2022). Numerical computation for gyrotactic microorganisms in MHD radiative Eyring–Powell nanomaterial flow by a static/moving wedge with Darcy–Forchheimer relation. *Micromachines*, 13(10), 1768.
- [18] Alwawi, F. A., Yaseen, N., Swalmeh, M. Z., & Qazaq, A. S. (2022). A computational numerical simulation of free convection catalysts for magnetized micropolar ethylene glycol via copper and graphene oxide nanosolids. Proceedings of the Institution of Mechanical Engineers, Part E: *Journal of Process Mechanical Engineering*, 09544089221146157.
- [19] Mamatha, S. U., Devi, R. R., Ahammad, N. A., Shah, N. A., Rao, B. M., Raju, C. S. K., ... & Guedri, K. (2023). Multi-linear regression of triple diffusive convectively heated boundary layer flow with suction and injection: Lie group transformations. *International Journal of Modern Physics B*, 37(01), 2350007.
- [20] Paullet, J. E., & Previte, J. P. (2020). Analysis of nanofluid flow past a permeable stretching/shrinking sheet. *Discrete & Continuous Dynamical Systems-Series B*, 25(11).
- [21] Swalmeh, M. Z., Shatat, F., Alwawi, F. A., Ibrahim, M. A. H., Sulaiman, I. M., Yaseen, N., & Naser, M. F. (2022). Effectiveness of radiation on magneto-combined convective boundary layer flow in polar nanofluid around a spherical shape. *Fractal and Fractional*, 6(7), 383..
- [22] Tlili, I., Ramzan, M., Nisa, H. U., Shutaywi, M., Shah, Z., & Kumam, P. (2020). The onset of gyrotactic microorganisms in MHD Micropolar nanofluid flow with partial slip and double stratification. *Journal of King Saud University-Science*, 32(6), 2741-2751.
- [23] Yaseen, N., Shatat, F., Alwawi, F. A., Swalmeh, M. Z., Kausar, M. S., & Sulaiman, I. M. (2022). Using micropolar nanofluid under a magnetic field to enhance natural convective heat transfer around a spherical body. *Journal of Advanced Research in Fluid Mechanics and Thermal Sciences*, 96(1), 179-193.
- [24] Song, Y. Q., Khan, S. A., Imran, M., Waqas, H., Khan, S. U., Khan, M. I., & Chu, Y. M. (2021). Applications of modified Darcy law and nonlinear thermal radiation in bioconvection flow of micropolar nanofluid over an off-centered rotating disk. *Alexandria Engineering Journal*, 60(5), 4607-4618.
- [25] Swalmeh, M. Z. (2021). Numerical solutions of hybrid nanofluids flow via free convection over a solid sphere. *Journal of Advanced Research in Fluid Mechanics and Thermal Sciences*, 83(1), 34-45.
- [26] Bidin, B., & Nazar, R. (2009). The numerical solution of the boundary layer flow over an exponentially stretching sheet with thermal radiation. *European Journal of scientific research*, 33(4), 710-717.
- [27] Ishak, A. (2011). MHD boundary layer flow due to an exponentially stretching sheet with radiation effect. *Sains Malaysiana*, 40(4), 391-395.
- [28] Dero, S., Rohni, A. M., & Saaban, A. (2019). MHD micropolar nanofluid flow over an exponentially stretching/shrinking surface: Triple solutions. *Journal of Advanced Research in Fluid Mechanics and Thermal Sciences*, 56(2), 165-174.
- [29] Alkasasbeh, H. (2022). Numerical solution of heat transfer flow of Casson hybrid nanofluid over a vertical stretching sheet with magnetic field effect. *CFD Letters*, 14(3), 39-52.

Contribution of Individual Authors to the Creation of a Scientific Article (Ghostwriting Policy)

- Feras Al Faqih, and Mohammed Swalmeh carried out the simulation and the optimization and implemented the Algorithm in MATLAB.
- Khuram Rafique, and Sehar Aslam have organized and executed the experiments and they prepared the final proof of the manuscript.

Sources of Funding for Research Presented in a Scientific Article or Scientific Article Itself

The corresponding author would like to acknowledge Al Hussein Bin Talal University for the financial support.

Conflict of Interest

The authors have no conflicts of interest to declare.

Creative Commons Attribution License 4.0 (Attribution 4.0 International, CC BY 4.0)

This article is published under the terms of the Creative Commons Attribution License 4.0

https://creativecommons.org/licenses/by/4.0/deed.en_US